International Journal of Physics and Research
Vol.1, Issue 1 (2011) 30-58
© TJPRC Pvt. Ltd.,

HEAT AND MASS TRANSFER OF AN MHD FORCED CONVECTION FLOW ALONG A STRETCHING SHEET WITH CHEMICAL REACTION, RADIATION AND HEAT GENERATION IN PRESENCE OF MAGNETIC FIELD

M.S. Hossain[1], M.A. Samand[2] and M.Mohebujjaman[3]
[1]Department of Natural Sciences
University of Information Technology and Sciences, Dhaka-1212, Bangladesh
[2]Department of Mathematics, University of Dhaka, Dhaka-1000, Bangladesh
[3]Department of Mathematics, Bangladesh University of Engineering and Technology, Bangladesh

ABSTRACT

The present study comprises of steady two dimensional magnetohydrodynamic heat and mass transfer forced convection flow along a vertical stretching sheet in the presence of magnetic field. The problem has been analyzed by applying Nachtsheim-Swigert shooting iteration technique with sixth order Runge-Kutta integration scheme. The nonlinear partial differential equations governing the flow fields occurring in the problems have been transformed to dimensionless nonlinear ordinary differential equations by introducing suitably selected similarity variables. The ensuing equations are simultaneously solved by applying numerical iteration scheme for velocity, temperature and concentration. The results are displayed graphically in the form of velocity, temperature and concentration profiles. The corresponding skin-friction coefficient, Nusselt number and Sherwood number are displayed graphically and also in tabular form as well. The effects of several important parameters on the velocity, temperature and concentration profiles are investigated.

KEY WORDS: Radiation parameter, electric conductivity, molecular diffusivity and Schmidt number.

INTRODUCTION

The concept of boundary allows simplifying the equation of fluid flow by dividing the flow field into two areas: one inside the boundary layer, where viscosity is dominant and the majority of the drag experienced by a body immersed in a fluid is created, and other outside the boundary layer where the viscosity can be neglected without significant effects on the solution. This allows a closed form solution for the flow in both areas, which is a significant simplification over the solution of the Navier-Stoke equations. The Navier-Stoke equations are time-dependent and consist of a continuity equation for conservation of mass, three conservation of momentum equations and conservation of energy equation. The majority of the heat transfers to and from a body also take places within the boundary layer. The thickness of the velocity boundary layer is normally defined as the distance from the solid body at which the flow velocity is 99% of the free stream velocity. The hydro-magnetic flow and heat transfer problems have become important industrially. To be more specific, it may be pointed out that many metallurgical processes involve the cooling of continuous strips or filaments by drawing them through a quiescent fluid and that in the process of drawing, these strips are sometimes stretched. In all the cases the properties of the final product depend on the rate of cooling to a great extent. By drawing such strips in an electrically conducting fluid subjected to a magnetic field, the rate of cooling can be controlled and a final product of desired characteristics can be achieved. Finally it can be said that the study of boundary layer flow and heat transfer over a continuously stretched surface is very important because of its various possible applications in countless places such as hot rolling, wire drawing and plastic extrusion, continuous casting, glass fiber production, crystal growing, paper production and many other places that

are important for our industrial developments and financial developments as well. Out of two types of convective heat and mass transfer, forced convection is the one where the velocity of flow dominates over the other parameters. Some kind of external forces are employed here. The cooling system in a car engine is an example of forced convection. Thermal radiation has a significant role in surface heat transfer, when convective heal transfer is similar. The radiation effect on forced and free convection have been studied in recent years extensively, as the magnetohydrodynamic [MHD] flow and heat transfer problems have become more important in many engineering and industrial applications. These include magnetohydrodynamic power generators, accelerators, and crystal growth. Mujtaba *et al.* [1] studied the effect of thermal radiation flow adjacent to a non-isothermal wedge in the presence of heat source or sink. Hossain and Takhar [2] studied thee radiation effects using the Rosseland diffusion approximation [3] that leads to non similar boundary layer equation governing the mixed convection flow of an optically dense viscous incompressible fluid past heated vertical plate with a free uniform velocity and surface temperature. Shateyi *et al.* [4] studied the thermal radiation and buoyancy effects on heat and mass transfer over a semi-infinite stretching surface with suction and blowing. Ali *et al.* [5] studied the radiation effect on natural convection flow over a vertical surface in a gray gas. Following Ali et al. Mansour [6] studied the interaction of mixed convection with thermal radiation in laminar boundary layer flow over a horizontal, continuous moving sheet with suction/injection. Azzam *et al.* [7] investigated the effects of radiation on the MHD mixed free-forced convective steady laminar boundary layer flow of an optically thick electrically conducting viscous fluid, past a moving semi-infinite vertical plate, for large temperature differences. Elbashbeshy *et al.* [8] studied the determination of the effect of radiation on forced convection flow of a micropolar fluid over a horizontal plate. Aydin *et al.* [9] investigated the mixed convection heat transfer about a permeable vertical plate in the presence of

magneto and thermal radiation effects. Cess [10] studied to determine the influence of radiation heat transfer upon the forced convection Nusselt number.Duwairi [11] worked to highlight the viscous and joule heating effects on forced convection flow in the presence of magneto and thermal radiation effect. Duwairi *et al.* [12] studied the MHD forced convection heat, transfer from radiate surfaces in the presence of a uniform transverse magnetic field with, conductive fluid suction or injection from a porous plate. Rahman *et al.* [13] analyzed a two dimensional steady MHD mixed convection and mass transfer flow over a semi-infinite porous inclined plate in the presence of thermal radiation with variable suction and thermophoresis. Samad and Rahman [14] investigated thermal radiation interaction with unsteady MHD flow past a vertical porous plate immersed in a porous medium. Samad and Karim [15] studied thermal radiation interaction with unsteady MHD free convection flow through a vertical flat plate with time dependent suction in the presence of magnetic field. Abo-eldahab [16] studied thermal radiation effects on MHD flow past a semi-infinite vertical inclined plate in the presence of mass diffusion. Mazumdar and Deka [17] studied the MHD flow past an impulsively started infinite plate in the presence of thermal radiation. Damesh [18] studied MHD mixed convection from radiate vertical isothermal surface embedded in a saturated porous media. As in the case of stretching sheets, Chen [19] studied laminar mixed convection adjacent to vertical continuously stretching sheet. Chiam [20] investigated MHD heal transfer over non-isothermal stretching sheet. Chiam [21] studied heat transfer in a stretching sheet with variable viscosity and variable heat transfer in stagnation point flow towards a lower stretching sheet. Seddeek *et al.* [23] studied laminar thermal diffusivity. Sharma and Mishra [24] studied steady MHD through horizontal channel, with the plate being a stretching sheet and the upper plate fluid with variable thermal conductivity over stretching sheet. Mahapatra *et al.* [22] investigated mixed convection adjacent to vertical continuously being a permeable plate bounded by

porous medium. Sriramalu *et al.* [25] investigated the steady flow and heat transfer of a viscous incompressible fluid flow through porous medium over a stretching surface. Pop *et al.* [26] studied radiation effect on the flow near the stagnation point of a stretching sheet. Sharma and Singh [27] studied the effects of variable thermal conductivity and heat source/ sink on MHD flow near a stagnation point on a linearly stretching sheet. Abo-eldahab [28] studied flow and heat transfer in a micropolar fluid past a stretching surface embedded in a non-Darcian porous medium with uniform free stream.

Mathematical Formulation

We consider a steady two-dimensional magneto hydrodynamic heat and mass transfer flow of a various incompressible fluid along a vertical stretching sheet with constant heat generation absorption with radiation. We take the X-axis along the sheet and Y-axis is normal to it. Two equal and opposite forces are introduced along the X-axis so that the sheet is stretched keeping the origin fixed. A uniformed magnetic field of strength B_0 is imposed along the Y-axis. A radiation depending on the temperature is applied on the stretching sheet. The physical configuration considered here is shown in the following Figure-1.

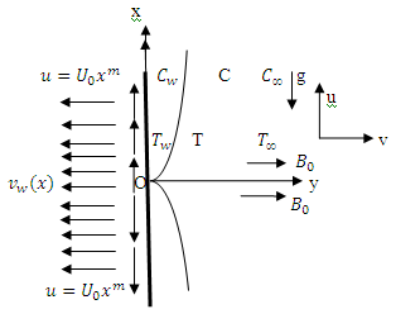

Figure 1: Flow model with coordinate system

To formulated the problem, at first the two dimensional continuity equation will be introduced. On the momentum boundary layer equation the left hand side consists of the acceleration terms. The right hand side consists of several terms. The first term indicates the viscous term, the second term indicates the buoyancy term which will be neglected for the force convection and the third term indicates the presence of magnetic field. On the energy equation, in addition with the usual terms a new term corresponding to radiation will have to be introduced in the right hand side referring to the radiative heat flux gradient. The corresponding equation consists of the usual terms.

Governing Equations

The governing equations representing the proposed flow field are:

Continuity equation:

$$\frac{\partial u}{\partial x}+\frac{\partial v}{\partial y}=0 \tag{1}$$

Momentum equations

$$u\frac{\partial u}{\partial x}+v\frac{\partial u}{\partial y}=\nu\frac{\partial^2 u}{\partial y^2}+sg\beta[T-T_\infty]-\frac{\sigma {B_0}^2}{\rho}u \tag{2}$$

Energy equation

$$u\frac{\partial T}{\partial x}+v\frac{\partial T}{\partial y}=\alpha\frac{\partial^2 T}{\partial y^2}+\frac{Q_0}{\rho c_p}(T-T_\infty)-\frac{1}{\rho c_p}\frac{\partial q_r}{\partial y} \tag{3}$$

Concentration equation

$$u\frac{\partial C}{\partial x}+v\frac{\partial C}{\partial y}=D_m\frac{\partial^2 C}{\partial y^2} \tag{4}$$

Where (u,v) are the velocity components along x and y directions respectively, ν is the kinematic viscosity of the fluid, g is the acceleration due to gravity, β is the volumetric co efficient of thermal expansion, B_0 is the uniform

magnetic field strength(magnetic induction), T and T_∞ are the fluid temperature within the boundary layer and in the free stream respectively, C is the concentration of the fluid within the boundary layer, ρ is the density of the fluid, C_p is the specific heat at constant pressure, α is the electrical conductivity, Q_0 is the volumetric rate of heat generation D_m is the Coefficient of mass diffusivity, q_r is the rate heat transfer and s is a dummy parameter stands for 0 for forced convection,+1 for heating problem and -1 for cooling problem.

Boundary conditions: The boundary conditions can be split into two parts. The first part is the wall boundary conditions and the second is the free stream conditions.

Boundary conditions:

$$u = u_w = U_0 x^m, v = v_w(x), C = C_w,$$

$$T - T_\infty = T_w - T_\infty = ax^n,$$

$$C - C_\infty = C_w - C_\infty = bx^1, C = C_w, \text{at } y = 0$$

$$u = 0, T \to T_\infty, \; C \to C_\infty \text{ at } y \to \infty$$

Here v_w is a velocity component at the wall having positive value to indicate suction. T_w is the uniform wall temperature and C_w, C_∞ are the concentration of the fluid at the sheet and far from the sheet respectively. The effect from second term on the right hand side of the equation (2) is due to buoyancy force and the governing equations (1)-(4) represent force convection flow when we take $s = 0$.

Similarity Analysis

To transform equations (2) to (4) into a set of ordinary differential equations the following dimensionless variables are introduced:

$$u = U_0 x^m f'(\eta) \tag{5}$$

$$\eta(x,y) = y\sqrt{\frac{m+1}{2}}\sqrt{\frac{U_0 x^m}{\nu x}} = y\sqrt{\frac{m+1}{2}}\sqrt{\frac{U_0 x^{m-1}}{\nu}} \tag{6}$$

$$T - T_\infty = a x^n \theta(\eta) \tag{7}$$

$$C - C_\infty = b x^l \varphi(\eta) \tag{8}$$

Where, η is the dimensionless distance normal to the sheet, f' is the dimensionless primary velocity, θ is the dimensionless fluid temperature and φ is the dimensionless concentration.

Finally we get the following local similarity equations:

$$f''' + ff'' - \frac{2m}{m+1}f'^2 - \frac{2M}{m+1}f' = 0 \tag{9}$$

$$\theta'' + \frac{3NPr}{3N+4}f\theta' + \frac{6NPr}{(m+1)(3N+4)}(Q - nf')\theta = 0 \tag{10}$$

$$\varphi'' + Scf\varphi' - \frac{2l}{m+1}Scf'\varphi = 0 \tag{11}$$

The transformed boundary conditions are:

$$\left.\begin{array}{l} f = f_w, f' = 1, \theta' = 1, \varphi' = 1 \text{ at } \square = 0 \\ f' = 0, \quad \theta = 0, \varphi = 0 \text{ at } \eta \to \infty \end{array}\right\} \tag{12}$$

Where a prime denotes differentiation with respect to η and $fw = -v_w\sqrt{\frac{2}{m+1}}\sqrt{\frac{x^{1-m}}{\nu U_0}}$ is the suction parameter.

The dimensionless parameters appeared into the above equations are defined as follows:

$Q = \frac{Q_0}{\rho c_p U_0} \frac{1}{x^{m-1}}$ is the Local rotation parameter

$M = \frac{\sigma \beta_0^2}{\rho} \frac{x^{1-m}}{U_0}$ is the local magnetic parameter

$N = \frac{\kappa \kappa_1}{4\sigma_1 T_\infty^3}$ is the radiation parameter and

$P_r = \frac{\mu c_p}{\kappa}$ is the Prandtl number

$Sc = \frac{\nu}{D_m}$ is the Schmidt number

Numerical Computations

The system of non-linear differential equations (9)-(11) with boundary conditions (12) have been solve numerically by using the aforesaid shooting iteration technique named after Nachtsheim-Swigert [29] (guessing the missing value) along with the Runge-Kutta sixth order iteration scheme. A step size of $\Delta\eta = 0.01$ has been used together with accuracy of 10^{-6} in all cases. The value of $\eta_{max}$was selected in accordance with the value of each group of parameters $Pr, f_w, M, N, Q, Sc, m, n, l$ to satisfy the accuracy requirement. The code verifying graphs for different step sizes are shown below.

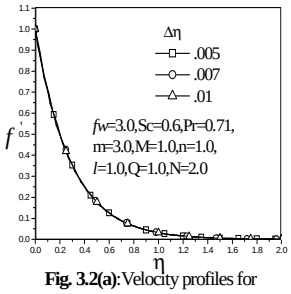

Fig. 3.2(a):Velocity profiles for various step sizes.

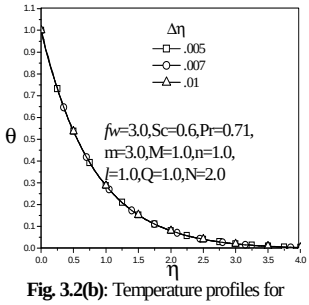

Fig. 3.2(b): Temperature profiles for various step sizes.

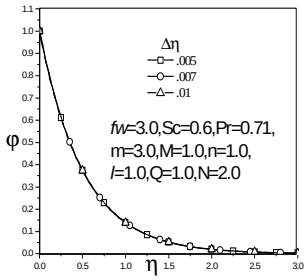

Fig. 3.2(c):Concentration profiles for various step sizes.

Here we see that for step sizes, $\Delta\eta = 0.01,\ 0.007,\ 0.005$ the velocity profiles, temperature profiles and the concentration profiles are good agreement among them.

RESULTS AND DISCUSSION

We have shown the dimensionless velocity, temperature and concentration profiles to present the results obtained in the numerical computations have been carried out for various values of parameters entering into the problem in compliance with the different physical conditions. These parameters are, the Prandtl number (Pr), suction parameter (f_w), magnetic field parameter (M),

radiation parameter (N), Schmidt number (Sc), heat source parameter (Q), velocity index (m), temperature index (n) and concentration index (l).

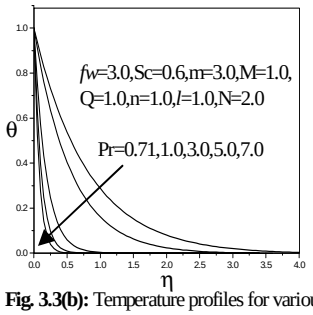

Fig. 3.3(b): Temperature profiles for various values of Prandlt number, Pr.

In **Fig. 3.3** the effects of Prandlt number (*Pr)*, on the velocity, temperature, and concentration profiles are shown. Here we see that there is no effect on velocity due to variation in the values of Prandlt numbers (*Pr).* This is because in the force convection the velocity is generally high in comparisons with the effect of Prandlt number *(Pr).* The momentum boundary layer thickness remains fixed with the increase of the Prandlt number (*Pr).* Thus there is no visible effect on the velocity profiles. So the velocity of the stretching sheet and the fluid particle remain same with the increase of the Prandlt number *(Pr).* On the other hand the temperature profiles show a sharp variation in **Fig. 3.3(b)** with the increase of Prandlt number (*Pr)* the decreases rate of the temperature increases. That is the heat transfer rate in the flow field increases with the increase of the Prandlt number *(Pr).* This is because, for lower Prandlt number *(Pr),* for example *Pr*=0.71, which represents the air, the heat transferred at much slower rate. On the other hand for *Pr*=7.0, which represents water at 20^0C, the heat transfer at much higher rate. The thermal boundary layer thickness decreases to a large extent with the increase of the Prandlt number. The concentration profiles show no variation due to the change in the Prandlt number (*Pr)* and have the same profile for all values of the Prandlt numbers. This is

because in the force convection the concentration is generally high in comparisons with the effect of Prandlt number. The concentration boundary layer thickness remains fixed with the increase of the Prandlt number *(Pr*). Thus there is no visible effect on the concentration profiles. It is inferred that the thickness of thermal boundary layer is greater for air (*Pr* = 0.71) and there is more uniform temperature profile across the thermal boundary layer as compared to water (*Pr* =7.0) and electrolyte solution (*Pr* =1.06). The reason is that smaller values of Prandtl number *(Pr)* are equivalent to increasing thermal conductivity and therefore heat is able to diffuse away from the heated surface more rapidly than for higher values of Prandtl number *(Pr)*. Thus temperature falls more rapidly for water than air and steam. For a high Prandtl number *(Pr),* the thermal boundary layer is larger than the momentum boundary layer. As a result, the velocity within the boundary layer is almost constant and temperature gradually decreases. Again For a high Prandtl number *(Pr),* the concentration boundary layer and the momentum boundary layer are almost same. So, the concentration within the boundary layer is almost constant.

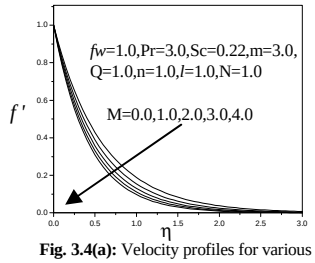

Fig. 3.4(a): Velocity profiles for various values of magnetic parameter, M.

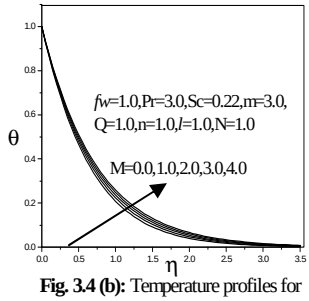

Fig. 3.4 (b): Temperature profiles for various values of magnetic parameter, M

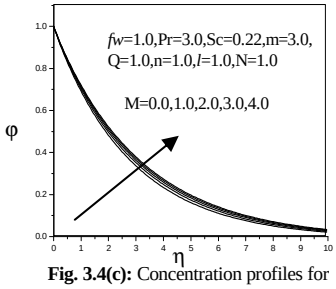

Fig. 3.4(c): Concentration profiles for various values of magnetic parameter, M.

In **Fig. 3.4** the effect of magnetic field parameter (*M)* is demonstrated. **Fig. 3.4(a)** shows that a variation occurs in the velocity profiles, that is, the rate of decrease, increases with the increase of the magnetic field parameter (*M).* It can be explained by the fact that the magnetic field produces a retarded action on the velocity field, thus decreasing the velocity at a higher rate. The momentum boundary layer thickness decreases slightly with the increase of the magnetic parameter *(M).* **Fig. 3.4(b)** shows a slight decrease in the decreasing rate of the temperature profiles. That is, the heat transfer rate decreases with the increase in the magnetic field strength. This is explained due to the retarding action of the magnetic field on the boundary layer causing the heat transfer rate getting slower and slower. This implies that the thermal boundary layer thickness increases a small amount with the increase of the magnetic parameter *(M).* The

concentration profiles in **Fig. 3.4(c)** also show a similar pattern of decreasing transfer rate due to the magnetic field effect.

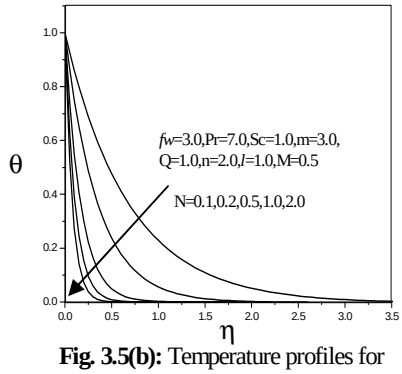

Fig. 3.5(b): Temperature profiles for various values of radiation parameter, N.

Fig. 3.5 shows the effect of radiation number *(N)* on the velocity, temperature, and concentration profiles. Since radiation is in the form of electromagnetic waves, no effects are seen on the velocity profiles**.** It is because of the higher velocity in the forced convection. The momentum boundary layer thickness remains fixed with the increase of the radiation parameter *(N)*. The temperature profiles show that, with the increase of radiation flux, the temperature in the vicinity of the boundary layer decreases more rapidly in **Fig. 3.5(b).** This can be explained easily by the fact that, with the increase of the radiation the heat transfer rate must increase. There is a large difference in the temperature profiles between the values 0.10 and 0.50 for (*N*). This is because, at the value of 0.10 the radiation is very negligible and upon reaching the value of 0.50, it becomes significant in the temperature field in the thermal boundary layer. With the increase of the radiation parameter (*N)* the thermal boundary layer thickness reduces very rapidly. The concentration profiles do not show any change in the variation of the radiation parameter (*N),* displayed in **Fig. 3.5(c).**

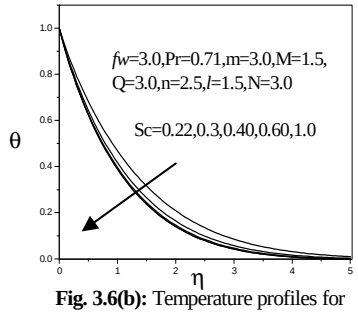

Fig. 3.6(b): Temperature profiles for various values of Schmidt number, Sc.

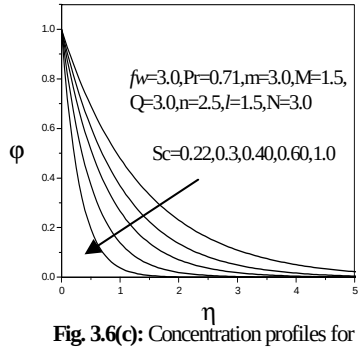

Fig. 3.6(c): Concentration profiles for various values of Schmidt number, Sc.

The effects of Schmidt number (Sc) are shown in **Fig. 3.6**. As usual there are no significant effects seen on the velocity**.** It is because of the higher velocity in the forced convection. The momentum boundary layer thickness remains fixed with the increase of the Schmidt number (Sc). The temperature profiles show that, with the increase of Schmidt number (Sc), the temperature in the vicinity of the boundary layer decreases more rapidly in **Fig. 3.6(b).** This can be explained easily by the fact that, with the increase of the Schmidt number (Sc) the heat transfer rate must increase. There is a large difference in the temperature profiles between the values 0.22 and 0.30 for Sc but very small difference for the values Sc are 0.40, 0.60 and 1.0. The thermal boundary layer thickness decrease with the increase of the Schmidt numbers (Sc). With the increase of the Schmidt

number (Sc) the thermal boundary layer thickness reduces very rapidly. The concentration profiles show a strong variation with the increase of Schmidt number (Sc) in **Fig. 3.6(c).** The decreasing rate of the concentration profiles increase to a large extent due to the increase in the Schmidt number (Sc). This is because with the increase of the Schmidt number (Sc) the kinematic viscosity increases and the mass diffusion coefficient decreases causing the concentration decrease rapidly.

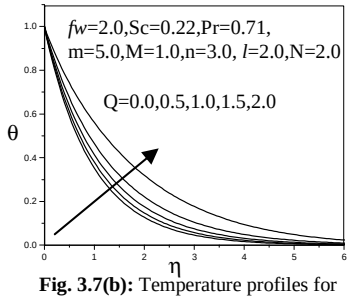

Fig. 3.7(b): Temperature profiles for various values of heat source parameter, Q.

Fig. 3.7 shows the heat source parameter (*Q)* effects on the flow field. The velocity profiles are almost unaffected**,** whereas, the temperature profiles show a decrease in the decreasing rate of heat source parameter (*Q)* in **Fig. 3.7(b)** in accordance with the physical requirements. The increase in the heat source parameter (*Q)* causes the temperature to decrease at a slower rate. This can be explained due to the fact that the heat source resists the temperature to decrease rapidly. In the case of a high heat source, for example, *Q* =7.0, the temperature rises at first and then decreases to the free stream temperature. The thermal boundary layer increases at a higher rate with the increase of the heat source parameter *(Q).* In the concentration profiles there is no significant change observed with the change in the heat source parameter (*Q).*

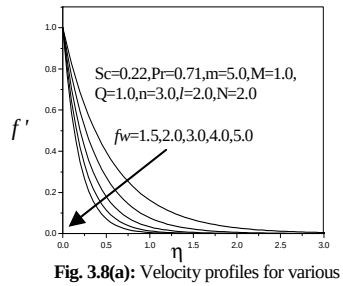

Fig. 3.8(a): Velocity profiles for various values of Suction parameter, fw.

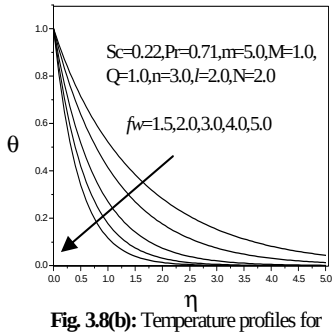

Fig. 3.8(b): Temperature profiles for various values of Suction parameter, fw.

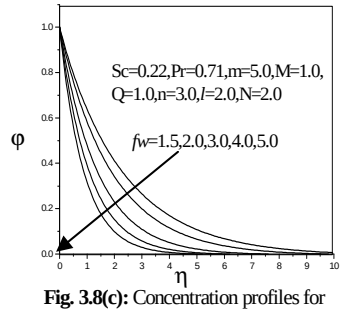

Fig. 3.8(c): Concentration profiles for various values of Suction parameter, fw.

In **Fig. 3.8** the effect of suction parameter (*fw*) is represented. We see that in all the three cases of velocity, temperature and concentration profiles there is sharp variation in the curves. The velocity profiles show an increase in their

decreasing rate with the increase of the suction parameter (*fw*), in **Fig. 3.8(a).** This can be explained by the fact that when the suction parameter (*fw*) increases, some of matter is removed from the system and the velocity gets retarded more rapidly. Also the momentum boundary layer thickness decreases with the increase of the suction parameter (*fw*) and thus reduces the chance of the boundary layer to the transition to turbulence. The temperature profiles in **Fig. 3.8(b)** shows also a decreasing trend with the increase of the suction parameter (*fw*). Thus it reduces the thermal boundary layer thickness with the increase of the suction parameter (*fw*) to a significant amount. The concentration profiles in the **Fig. 3.8(c)** show a large variation on the effect of suction parameter (*fw*). As the two other cases the concentration profiles also show a large amount of decreasing trend with the increase of the suction parameter (*fw*).

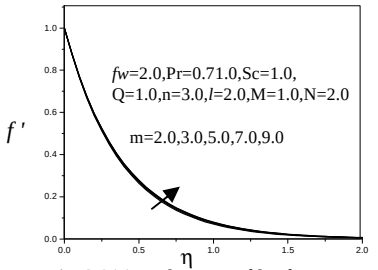

Fig. 3.9(a): Velocity profiles for various values of velocity index, m.

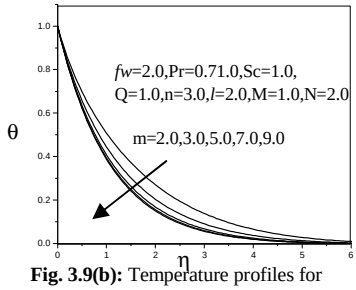

Fig. 3.9(b): Temperature profiles for various values of velocity index, m.

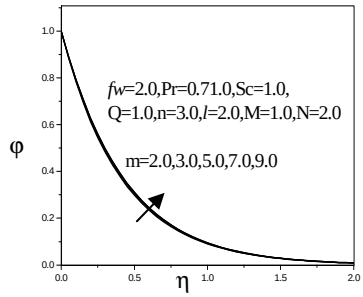

Fig. 3.9(c): Concentration profiles for various values of velocity index, m.

In **Fig. 3.9** the effect of velocity index (***m)***, is demonstrated. **Fig. 3.9(a)** shows that a variation occurs in the velocity profiles, that is, the rate of increase; small increases with the increase of the velocity index, (***m).*** It can be explained by the fact that the velocity index produces a retarded action on the velocity field, thus decreasing the velocity at a small rate. The momentum boundary layer thickness decreases slightly with the increase of the velocity index (***m)***. Fig. **3.9(b)** shows a slight increase in the decreasing rate of the temperature profiles. That is, the heat transfers rate increase with the increase in the velocity index (*m*). This is explained due to the retarding action of the velocity index (*m*) on the boundary layer causing the heat transfer rate getting slower and slower. This implies that the thermal boundary layer thickness decrease a small amount with the increase of the velocity index (*m*). The concentration profiles in the **Fig. 3.9(c)** also show a similar pattern of increasing transfer rate due to the velocity index (*m*) effect.

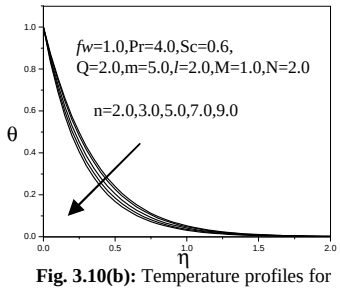

Fig. 3.10(b): Temperature profiles for various values of temperature index, n.

.**Fig. 3.10** shows the temperature index, (***n)*** effects on the flow field. The velocity profiles are almost unaffected**,** whereas, the temperature profiles show a increase in the decreasing rate of heat source in **Fig. 3.10(b)** in accordance with the physical requirements. The increase in the temperature index, (***n)*** causes the temperature to increase at a slower rate. This can be explained due to the fact that the temperature index (***n***) resists the temperature to decrease rapidly. In the case of a high temperature index (***n***), for example, ***n***=9.0, the temperature rises at

first and then decreases to the free stream temperature. The thermal boundary layer decreases a great amount with the increase of the temperature index (***n***). In the concentration profiles there is no significant change observed with the change in the heat temperature index (***n***).

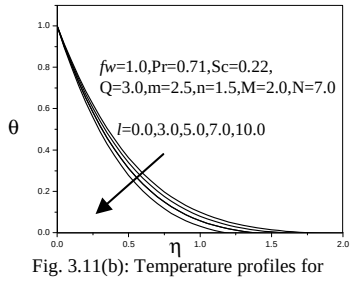

Fig. 3.11(b): Temperature profiles for various values of concentration index, l.

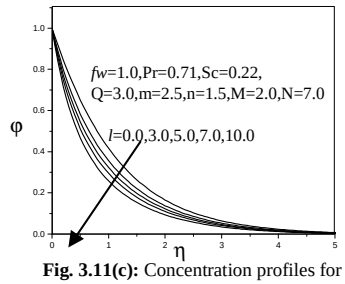

Fig. 3.11(c): Concentration profiles for various values of concentration index, l.

Fig. 3.11 the effect of concentration index (***l)*** is represented. We see that the cases of temperature and concentration profiles there is sharp variation in the curves.. The velocity profiles are almost unaffected and the momentum boundary layer thickness remains fixed with the increase of the concentration index (***l***).The temperature profiles in **Fig. 3.11 (b)** shows also a decreasing trend with the increase of the concentration index (***l)***. Thus it reduces the thermal boundary layer thickness with the increase of the concentration index (***l***) to a significant amount. The concentration profiles in **Fig. 3.11(c)** show a large variation on the effect of concentration index (***l)***. As the second case the

concentration profiles also show a large amount of decreasing trend with the increase of the concentration index (***I***).

Skin-friction coefficients, the Nusselt number and the Sherwood number:

The skin friction coefficients, (C_f) the Nusselt number (Nu_x) and the Sherwood number (Sh) are significant in the engineering field .These parameters refer to the wall shear stress, local wall heat transfer rate and wall mass transfer rate respectively.

The equation defining skin frictions is:

$$C_f = \sqrt{2(m+1)}Re_x^{-\frac{1}{2}}f''(0) \tag{13}$$

The local Nusselt number Nu_x is given by:

$$Nu_x = -\sqrt{\frac{m+1}{2}}\sqrt{Re_x}\,\theta'(0) \tag{14}$$

The local Sherwood number (Sh) is given by

$$:Sh = -\sqrt{\frac{m+1}{2}}\sqrt{Re_x}\,\varphi'(0) \tag{15}$$

Where, $Re_x = \frac{u_{0\infty}{}^{m+1}}{\nu}$ is the local Reynolds number and $\frac{1}{\sqrt{2(m+1)}}$, $\sqrt{\frac{2}{m+1}}Re_x^{-\frac{1}{2}}$, $\sqrt{\frac{2}{m+1}}Re_x^{-\frac{1}{2}}$ are constant.

It is observed from equations (13) to (15) that the Skin-friction coefficient, Nusselt number and the Sherwood number are proportional to $f''(0), -\theta'(0),$ and $-\varphi'(0)$ respectively.

Table 3.1: C_f, Nu_x and Sh for different values of Pr, M and N

Pr	C_f	Nu_x	Sh	M	C_f	Nu_x	Sh	N	C_f	Nu_x	Sh
0.71	-4.3996	1.7515	3.1013	0.0	-1.7379	1.4734	0.3843	0.10	-3.4392	1.5063	3.2252
1.0	-3.5032	1.8118	1.9676	1.0	-2.7321	1.1496	1.6209	0.20	-3.4398	2.8757	3.2263
3.0	-3.5032	5.5373	1.9687	2.0	-2.6878	0.82	1.5366	0.50	-3.4404	5.9737	3.2273
5.0	-3.5032	9.1915	1.9687	3.0	-2.665	0.903	1.4928	1.0	-3.4404	9.3091	3.2273
7.0	-3.5032	12.8221	1.9687	4.0	-2.3846	1.3319	0.3464	2.0	-3.4404	12.9495	3.2273

Table 3.2: C_f, Nu_x and Sh for different values of f_w, Q and Sc

f_w	C_f	Nu_x	Sh	Q	C_f	Nu_x	Sh	Sc	C_f	Nu_x	Sh
1.5	-2.2557	0.7141	0.4716	0.0	-2.6415	1.0855	0.5604	0.22	-3.5651	0.8183	0.7535
2.0	-2.6415	0.9342	0.5604	0.5	-2.6415	1.0166	0.5604	0.30	-3.5651	0.9297	1.0183
3.0	-3.4831	1.3483	0.7511	1.0	-2.6415	0.9342	0.5604	0.40	-3.5651	0.9746	1.3448
4.0	-4.3825	1.7619	0.9528	1.5	-2.6415	0.8258	0.5604	0.60	-3.5651	0.9899	1.9902
5.0	-5.3148	2.1785	1.1607	2.0	-2.6415	0.6419	0.5601	1.00	-3.5651	0.9899	3.2571

Table 3.3: C_f, Nu_x and Sh for different values of m, n and l

m	C_f	Nu_x	Sh	n	C_f	Nu_x	Sh	l	C_f	Nu_x	Sh
2.0	-2.6878	0.82	2.4576	2.0	-1.9032	2.6979	0.9616	0.0	-1.9391	1.7947	0.8206
3.0	-2.665	0.903	2.3979	3.0	-1.9032	2.8619	0.9616	3.0	-1.9391	1.8944	1.152
5.0	-2.6415	0.943	2.3365	5.0	-1.9032	3.1675	0.9616	5.0	-1.9391	2.0096	1.3501
7.0	-2.6296	0.9555	2.3051	7.0	-1.9032	3.4479	0.9616	7.0	-1.9391	2.0095	1.5332
9.0	-2.6223	0.9609	2.2861	9.0	-1.9032	3.7078	0.9616	10.0	-1.9391	2.1507	1.7857

Wrapping up the above elucidations we can make the following conclusions:

1. In the forced convection the velocity being large, the Prandtl number (Pr) has no effective dominance over velocity and concentration. Nevertheless

the temperature it has a significant effect. With the increase of Prandtl number (Pr) the local heat transfer rate increases.

2. The radiation parameter (N) has a large effect on the temperature profiles, and hence can be used effectively to control the temperature of the flow field.

3. The magnetic parameter (M) has significant effect on the velocity, temperature and concentration profiles. So, magnetic field can effectively be used to control the flow field.

4. As apparent the temperature increases within the boundary layer with the increase of the heat source parameter (Q).

5. For the increase of the suction parameter (f_w) the velocity, temperature and concentration significantly decrease and as a consequence making it one of the most essential parameter in the boundary layer control theory.

6. The Schmidt number (Sc) has large effects on the concentration profiles dominating the mass transfer rate of the flow.

7. The velocity index (m) has significant effect on the velocity, temperature and concentration profiles.

8. The temperature index (n) has large effects on the temperature profiles dominating the mass transfer rate of the flow.

9. The concentration index (l) has significant effect on the temperature and concentration profiles. So, concentration index (l) can effectively be used to control the flow field.

ACKNOWLEDGEMENT

I express my gratitude to the Department of Mathematics, University of Dhaka to support and providing us the computer lab facilities.

NOMENCLATURE

B_0	Uniform magnetic field strength
C	Species concentration in the flow field
C_w	Species concentration at the wall
C_∞	Species concentration in the free stream
C_f	Skin friction coefficient
c_p	Specific heat at constant pressure
D_m	Coefficient of mass diffusivity
f	dimensionless stream function
fw	Suction parameter
Gr	Grashof number
g	acceleration due to gravity
κ	Thermal conductivity
κ_1	Mean absorption coefficient
l	Concentration index
M	Magnetic field parameter
m	Velocity index
N	Radiation parameter
n	Temperature index
Nu_x	Local Nusselt number
Pr	Prandtl number
Q_0	Heat source parameter
Q	Heat source parameter

q_r Radiative heat flux (Rosseland approximation)

Re Reynolds number

Re_x Local Reynolds number

Sc Schmidt number

Sh Sherwood number

T Temperature within the boundary layer

T_w Temperature at the wall

T_∞ Free stream temperature

u Velocity along x-axis

v Velocity along y-axis

v_w Suction velocity

x Coordinate along the plate

y Coordinate normal the plate

Greek symbols

α Thermal diffusivity

β Volumetric coefficient of thermal expansion

η Similarity variable

$\Delta\eta$ Step size

θ Dimensionless fluid temperature

μ Coefficient of viscosity

ν Coefficient of kinematics viscosity

ρ Fluid density

σ Electrical conductivity

φ Dimensionless fluid concentration Subscript

ψ Stream function

∞ Outside the boundary layer condition superscript

$'$ Differentiation with respect to η

REFERENCES

1. Mujtaba. M., Chamkha, A.J., Issa, Camille. "Thermal Radiation Effects on MHD Forced Convection Flow Adjacent to a Non-Isothermal Wedge in the Presence of a Heat Source or Sink". *Heat and Mass Trans.* Vol 39, Pp 305-312, 2003.
2. Hossain, M. A., Takhar, H. S. "Radiation Effect on Mixed Convection along a Vertical Plate with Uniform Surface Temperature". *Heat and Mass Trans.* Vol 31(4), Pp 243-248, 1996.
3. Seigel, R., Howell, J. R. "Thermal Radiation Heat Transfer". *McGraw-Hill New York* 1972.
4. Shateyi, S. Petersen, M. "Thermal Radiation and Buoyancy Effects on Heat and Mass Transfer over a Semi-Infinite Stretching Surface with Suction and Blowing". *J. Appl. Math.* Vol 2008, 12 Pages, 2008.
5. Ali, M. M., Chen, T. S. And Armaly , B. F. "Natural Convection Radiation Interaction In Boundary Layer Flow over Horizontal Surfaces". *AIAA Journal*, Vol 22(12), Pp 797-803, 1984.
6. Mansour, M. A. "Radiative and Free Convection Effects on the Oscillatory Flow past a Vertical Plate". *Astrophysics Space Sci.* Vol 166, Pp 269-275, 1990.
7. Azzam, A., El-Din, G. "Thermal Radiation Effect On MHD Mixed Free-Forced Convection Flow Past a -Semi-Infinite Moving Vertical Plate for High Temperature Differences". *Physica Scripta.* Vol 66, Pp 71-76.
8. Elbashbeshy, E. M. A. Bazid, M. A. A. "Effect of Radiation on Forced Convection Flow of a Micropolar Fluid over a Horizontal Plate". *Can. J. Phys.* Vol 78, Pp 907-913, 2000.

9. Aydin, O., Kaya. A. “Radiation Effect On MHD Mixed Convection Flow About A Permeable Vertical Plate”. *Heat Mass Trans.* Vol 45, Pp 239-246, 2008.
10. Cess, R. D. “The Effect of Radiation upon Forced Convection Heat Transfer”. *Appl. Sci. Res. Sec A.* Vol 10, Pp l269-1277, 1966.
11. Duwairi, H. M. “Viscous and Joule Heating Effects on Forced Convection Flow from Radiate Isothermal Porous Surfaces”. *Int. J. Numerical Methods for Heat & Fluid Flow.* Vol *15, Issues,* Pp 429-440, 2005.
12. Duwairi, H, M., Damesh, R. A., Al-Odat, M. “Similarity Analysis of Magnetic Field and Thermal Radiation Effects on Forced Convection Flow”. *Turkish J. Eng. Env. Sci.* Vol 30, Pp 83-89, 2006.
13. Rahman, M. M. , Alam, M. S. , Satter, M. A. , “Effect of Variable Suction and Thermophoresis on Steady MHD Combined Free-Forced Convective Heat and Mass Transfer Flow over a Semi-Infinite Permeable Inclined Plate in the Presence of Thermal Radiation”. *Int. J. Therm. Sci.* Vol 47(6), Pp 758-765, 2008.
14. Samad, M. A., Rahman. M. M. “Thermal Radiation Interaction with Unsteady MHD Flow past a Vertical Porous Medium”. *J. Nav. Arch. Mar. Eng.* Vol 3, Pp 7-14, 2006.
15. Samad, M. A., Karim. M. E. “Thermal Radiation Interaction with Unsteady MHD Flow past a Vertical Flat Plate with Time Dependent Suction”. *Dhaka Univ. J. Sci.* Vol 57(1), Pp 113-118, 2009.
16. Abo-EIdahab, E. M. “Thermal Radiation Effects on MHD Flow past a Semi-Infinite Vertical Inclined Plate in The Presence of Mass Diffusion”. *Canadian J. Phy.* Vol 83. Pp 243-256, 2005.
17. Mazumdar, M. K. Deka, R. K. “MHD flow past an Impulsively Started Infinite Vertical Plate in Presence of Thermal Radiation”. *Rom. J. Phvs.* Vol 52, Pp 565-573, 2007

18. Damesh, R. A. "MHD Mixed Convection From Radiate Vertical Isothermal Surface Embedded in a Saturated Porous Media". *Tran. ASME, J. Appl. Math.* Vol 73, Pp 54-59, 2006.
19. Chen, C. H. "Laminar Mixed Convection Adjacent to Vertical, Continuously Stretching Sheet". *Heat and Mass Tran.* Vol 33, Pp 471-476, 1998.
20. Chiam, T. C. "Magnetohydrodynamic Heat Transfer over a Non-Isothermal Stretching Sheet". *Acta Mechanica*, Vol 122, Pp 169-179, 1997.
21. Chiam, T. C. "Heat Transfer in a Fluid with Variable Thermal Conducting over Stretching Sheet". *Acla Mechanica*, Vol 129, Pp 63-72, 1998.
22. Mahapatra, T. R., Gupta, A. S. "Heat Transfer in Stagnation Point Flow Towards a Stretching Sheet". *Heat and Mass Tran.* Vol 38, Pp 517-521, 2002.
23. Seddeek, M. A., Salem, A. M. "Laminar Mixed Convection Adjacent to Vertical Continuously Stretching Sheet with Variable Viscosity and Variable Thermal Diffusivity". *Heat & Mass Tran.* Vol 41, Pp 1048-1055, 2005.
24. Sharma, P. R., Mishra, V. "Steady MHD Flow Through Horizontal Channel: Lower Being a Stretching Sheet and Upper Being a Permeable Plate Bounded By Porous Medium". *Bull. Pure Appl. Sci.* Vol *20E*, Pp 175-181, 2001.
25. Sriramalu, A. Kishan N., Anand, R. J. "Steady Flow and Heat Transfer of a Viscous Incompressible Fluid Flow through Porous Medium over a Stretching Sheet". *J. Energy, Heat & Mass Tran.* Vol 23, Pp 483-495, 2001,
26. Pop. S.R., Grosan, T., Pop, I. "Radiation Effect on the Flow near the Stagnation Point of a Stretching Sheet". *The Chnische Mechanik*, Vol 25, Pp 100-106, 2004.

27. Sharma, P. R. Singh, G. “Effect of Variable Thermal Conducting and Heat Source/Sink on MHD Flow Near a Stagnation Point on a Linearly Stretching Sheet”. *J. Appl. Fluid. Mech*. Vol 2. Pp 13-21, 2009.
28. Abo-EIdahab, E. M. “Flow And Heat Transfer in a Micropolar Fluid past a Stretching Surface Embedded in a Non-Darcian Porous Medium with Uniform Free Stream”. *Appl. Math. Comp*. Vol 162, Pp 881-889, 2005.
29. Nachtsheim, P. R., Swigert, P. “Satisfaction of the Asymptotic Boundary Conditions in Numerical Solution of the System of Non-Linear Equations of Boundary Layer Type”. *NASA TND*-3004, 1965.